Environmental Modelling and Software 118 (2019) 211–225

Contents lists available at ScienceDirect

Environmental Modelling & Software

journal homepage: www.elsevier.com/locate/envsoft

An evaluation of HSPF and SWMM for simulating streamflow regimes in an urban watershed

Mohammad Nayeb Yazdi[a], Mehdi Ketabchy[b], David J. Sample[c,*], Durelle Scott[a], Hehuan Liao[a]

[a] Department of Biological System Engineering, Virginia Polytechnic Institute and State University, Blacksburg, VA, USA
[b] Water Resources Engineer, Gannett Fleming, Inc., Fairfax, VA, USA
[c] Department of Biological System Engineering, Virginia Polytechnic Institute and State University, Hampton Roads Agricultural Research and Extension Center, Virginia Beach, VA, USA

ARTICLE INFO

Keywords:
HSPF
SWMM
Streamflow
Baseflow
Peak flow
Sensitivity analysis

ABSTRACT

Hydrologic models such as the Storm Water Management Model (SWMM) and the Hydrologic Simulation Program-Fortran (HSPF) are widely used to evaluate the impacts of urban development on watersheds and receiving waters. We compare the ability of these two models at simulating streamflow, peak flow, and baseflow from an urban watershed. The most sensitive hydrologic parameters for HSPF were related to groundwater; for SWMM, it was imperviousness. Both models simulated streamflow adequately; however, HSPF simulated baseflow better than SWMM, while, SWMM simulated peak flow better than HSPF. Global Sensitivity Analysis showed that variability of streamflow for SWMM was higher than that of HSPF, while variability of baseflow for HSPF was greater than that of SWMM. Further, analysis of extreme storm events indicated that the runoff coefficient for SWMM was slightly greater than HSPF for recurrence intervals of 1, 2, 5, and 10-yr.; the opposite was the case for recurrence intervals greater than 10 yrs.

1. Introduction

Urbanization alters watershed hydrology by increasing imperviousness and channelizing or piping natural drainageways (Hester and Bauman, 2013; Li et al., 2013; Liu et al., 2015). These changes reduce infiltration, increase runoff volume, accelerate the time to runoff peak (lag time), and reduce baseflow to streams (Chen et al., 2017; Lacher et al., 2019; Locatelli et al., 2017; Rosburg et al., 2017). Increasing runoff volume results in higher streambank and channel erosion (Whitney et al., 2015; Yousefi et al., 2017). Increases in peak runoff and decreasing lag time increases flooding (Roodsari and Chandler, 2017; Zope et al., 2016), damaging public or private property. Urbanization also leads to higher sediment and nutrient loads delivered to downstream water bodies. causing eutrophication and degrading water quality, threatening aquatic ecosystems (Daghighi, 2017; Liu et al., 2018; Luo et al., 2018; Stoner and Arrington, 2017). A variety of stormwater control measures (SCMs) also known as best management practices (BMPs) have been developed for mitigating urban impacts. Historically, management of urban runoff meant mitigating peaks using storage; this practice has given way to a more holistic focus on the restoration of the natural hydroperiod; known as low impact development (LID) or green stormwater infrastructure (GSI). SCMs that assist in these goals tend to focus on infiltration (Golden and Hoghooghi, 2017; Liu et al., 2018; Lucas and Sample, 2015).

Watershed models are used to: (1) simulate hydrology and water quality in runoff, streams, and water bodies; (2) evaluate the impacts of urban development; and (3) investigate effectiveness of watershed restoration strategies (Borah et al., 2019; Niazi et al., 2017). While numerous watershed models exist, limited information is available to guide in their selection. Two commonly used watershed models include the U.S. Environmental Protection Agency's (USEPA) Storm Water Management Model (SWMM) (USEPA, 2018), and the Hydrologic Simulation Program-Fortran (HSPF) (USEPA, 2014). SWMM is a dynamic/physically-based hydrologic and hydraulic model which is used to simulate runoff quantity and quality during discrete events and continuous periods (Huber and Dickinson, 1988; James et al., 2010; Rossman, 2010). SWMM is often used in urban areas because it is capable of simulating conveyance systems. HSPF is a comprehensive process-based watershed model that simulates watershed hydrology and water quality (Bicknell et al., 2001; Linsley et al., 1975). Both SWMM and HSPF were developed by the USEPA. HSPF has been applied across large, regional watersheds, such as the Chesapeake Bay

* Corresponding author. Hampton Roads Agricultural Research and Extension Center, Virginia Polytechnic Institute and State University, 1444 Diamond Springs Rd, Virginia Beach, VA, 23455, USA.
E-mail address: dsample@vt.edu (D.J. Sample).

https://doi.org/10.1016/j.envsoft.2019.05.008
Received 25 January 2019; Received in revised form 28 March 2019; Accepted 10 May 2019
Available online 16 May 2019
1364-8152/

watershed, a 166,000 km^2 watershed (USEPA, 2010). The HSPF-based Chesapeake Bay watershed model discretizes subwatersheds based upon HUC-12 (hydrologic unit code) watershed delineations and geopolitical considerations, such as City, County, and State boundaries (Shenk et al., 2012). Due to the complexity inherent in urban storm drainage networks and their "flashy" runoff, SWMM models tend to be used at smaller scales to capture this response (Niazi et al., 2017).

Recent (< 10 years) published research based upon use of SWMM or HSPF that used at least two statistical methods for evaluating model performance were compiled in Table 1. Based on the references provided in Table 1, SWMM has been applied to watershed ranging in size from 2 ha to 40,000 km^2, however, it has primarily been used within smaller urban watersheds (< 2 km^2). SWMM has specific functionality for simulation of SCMs and LID, incorporating a variety of physical processes such as storage routing and infiltration. On the other side, HSPF has also been applied across a wide range of larger watersheds (3–70,000 km^2). Although HSPF has been applied to urban watersheds, it has several limitations; HSPF does not directly simulate conveyance systems, nor does it directly simulate SCMs. HSPF models SCMs by shifting some of the watershed area's land use from urban to undeveloped and changing the F-tables, as these govern stream dimensions in the HSPF model (Dudula and Randhir, 2016; Mohamoud et al., 2010; U.S.EPA, 2014). The lack of explicit SCM representation is a key weakness of HSPF (Mohamoud et al., 2010). HSPF is typically based upon readily available spatial data and must be calibrated to monitoring data. In contrast, SWMM depends upon physically based parameters that are collected or derived from spatial data gathered at smaller scales.

A comparative assessment of HSPF and SWMM in simulating hydrology of watersheds has been conducted only in a few studies; both were conducted in forested, not urban watersheds Lee et al. (2010) compared SWMM output with average streamflow from a large watershed during seven events. The authors indicated that both models performed adequately; however, HSPF simulated hourly streamflow better than SWMM. Tsai et al. (2017) applied SWMM and HSPF to a highly pervious, forested watershed. The authors indicated that HSPF matched observed streamflow better than SWMM. This may have been due to the highly permeable soil of the watershed which likely created a strong baseflow response. A key application of HSPF is the simulation of hydrology and water quality of the Chesapeake Bay watershed (USEPA, 2010). This is directly the result of HSPF's simplicity, which allows HSPF to execute simulations of this large watershed faster. This computational advantage is evident in execution of large watershed models for long times. SWMM's advantages are its ability to simulate "flashy" urban watersheds and assess SCM performance. As both models are widely used in urban areas, understanding the similarities and differences between them is critical, yet a comprehensive comparison has not been done.

The objective of this paper was to address this research need by comparing the capabilities of HSPF and SWMM as applied to a case study urban watershed. HSPF and SWMM were each assessed in terms of the (1) most sensitive hydrologic parameters in the watershed, (2) simulation of daily and monthly streamflows in comparison with observed data, (3) simulation of peak flows, baseflows and their respective durations, and (4) predicted runoff coefficients during storm events with set return periods. These results were then used to compare the subcomponents of the long-term watershed hydrograph. Achieving a better understanding of the similarities and differences of SWMM and HSPF will help relate information from each model to the other, which will assist in meeting water quality goals at the regional scale.

2. Materials and methods

2.1. Site description

Stroubles Creek, located within Montgomery County, Virginia, lies within the Valley and Ridge physiographic province of Virginia. Stroubles Creek is a tributary to the New River, which is tributary to the Kanawha River, and part of the Mississippi River basin. An urbanized, 14.8-km^2 headwater portion of the Stroubles Creek watershed was selected for this study (Fig. 1). This subwatershed includes much of downtown Blacksburg and the campus of Virginia Polytechnic Institute and State University (Virginia Tech). This watershed was selected because: 1) its headwaters are predominately (73.8%) urbanized, and 2) long-term monitoring data are available. The Virginia Tech Stream, Research, Education, and Management (StREAM) Lab (StREAM Lab, 2009) continuously measures groundwater levels, streamflows, and records precipitation and other climatological data within the Stroubles Creek watershed. Land cover is 73.8% urban (with a total imperviousness of 32%), 21% agricultural, 4% forested, and 1.2% water body (Multi-Resolution Land Use Consortium, 2011) (Fig. 1). The dominant Hydrologic Soil Group (HSG) of the headwaters is category C as classified by the Natural Resource Conservation Service (NRCS, 2007, 1999a), while downstream consists mainly of silt loam and loam soils, which are category B (Mostaghimi et al., 2003). The average elevation of the watershed is 670 m above sea level. Mean annual precipitation is 1030 mm (Hofmeister et al., 2015; Liao et al., 2015).

2.2. Data collection

Storm sewer, street, parcel boundary, and surface elevation geographic information system (GIS) data were provided by the Town of Blacksburg (Town of Blacksburg, 2015) and Virginia Tech; separate datasets were merged. Soil information was obtained from the Soil Survey Geographic Database (SSURGO) of the Natural Resources Conservation Service, with scales ranging from 1:12,000 to 1:64,000 (NRCS, 1999b). The monitoring station measures stream stage every 15 min using a pressure transducer (CS451, Campbell Scientific Inc., Logan, UT, USA), with a water level resolution of 0.0035% FS (Full Scale/Full Span, the difference between the lowest and highest measured point) and a CR1000 datalogger (Campbell Scientific Inc., U.S). Stage was converted to discharge using a rating curve computed through the historical monitoring of stage-flow. Precipitation was recorded at 15-min intervals at the StREAM Lab metrological station using a tipping bucket rain gages (TR-525USW, Texas Electronics, Inc., Dallas, TX, ± 1%). The StREAM Lab weather station measured air temperature every 30 min at the approximately 300 m downstream of the Stroubles Creek monitoring station. StREAM Lab and the meteorological station are located at the watershed outlet. The depth to surficial groundwater was measured every 10 min by two piezometers installed in the floodplain adjacent to StREAM Lab using two CS451 water level loggers (Campbell Scientific, U.S). Groundwater table elevation was quantified using geological maps of Geology and Mineral Resources Division of Commonwealth of Virginia (Appendix A), and data from the StREAM Lab pre-installed floodplain piezometers.

2.3. Model initialization

Land cover data was initially used to initialize the models in a process described by Ketabchy (2018). The principal input parameters used in development of the HSPF and SWMM models were land use, soil properties, stream characteristics, and time series of precipitation and temperature. A total of 43 subwatersheds were delineated within the Stroubles Creek watershed. The watershed was delineated through ArcGIS 10.5 (Ketabchy et al., 2018), correcting the delineation for urban features (i.e. topography, slope, elevation, land use, etc.) where necessary. The differences and similarities of each process feature and main input/output variables for HSPF and SWMM are summarized in Table 2.

SWMM uses a simplified Darcy's law to simulate groundwater flows and interaction of surface water and groundwater of an aquifer through a number of parameters: bottom elevation of aquifer, groundwater-surface water interaction parameters (A_1, A_2, B_1, and B_2, which are

Table 1
Summary of recent studies in simulation hydrology and water quality of watersheds by using SWMM and HSPF (sorted by watershed size).

Reference	Catchment area (km^2)	Indicator	[a] LID simulation	Simulation period	Frequency of data	Streamflow Model performance			Descriptions/Results
						[b] R^2	[c] NSE	[d] PBIAS	
SWMM									
Rai et al. (2017)	39269	Peak flows	–	1980 to 2012	Monthly	–	0.66	−14%	Using SWMM model for simulating the catchment response to flood events
Alamdari et al. (2017)	150	Streamflow, peak flow, [e] TSS, [f] TN, [g] TP	–	2010 to 2013	Hourly	0.78	0.73	12.1%	Effect of climate change on hydrology and water quality of the watershed.
Moore et al. (2017)	1.5	Streamflow, peak flow, groundwater elevation	–	2013 to 2014	30 min	0.6	–	−38.7%	Modeling Highway Stormwater Runoff and Groundwater with SWMM
Guan et al. (2015)	0.12	Peak flows	Rain barrel, permeable pavement	2001 to 2006	30 min	0.84	0.9	–	Modeling and assessment of hydrological changes in a developing urban catchment
Palla and Gnecco (2015)	0.06	Runoff, peak flow, streamflow	Green roof, permeable pavement	7 events in 2005	One minute	–	0.84	−2%	Hydrologic modeling of LID systems at the urban catchment scale
Nayeb Yazdi et al., (2019b)	0.05	Runoff, TSS, TN, TP	–	2017 to 2018	15 min	0.71	0.69	19%	
Rosa et al. (2015)	0.02	Runoff	Rain garden, permeable pavement, bioretention	2003 to 2005	15 min	0.8	0.68	–	Calibration and Verification of SWMM for Low Impact Development
HSPF									
Stern et al. (2016)	68000	Streamflow, sediment load	–	1958 to 2008	Daily	0.75	0.66	−15%	Impact of climate change on streamflow and sediment load.
Huiliang et al. (2015)	6700	Streamflow, TP, TN	–	2004 to 2010	Daily	0.82	0.79	10.4%	Modeling NPS pollution in the watershed
Tong et al. (2012)	5840	Streamflow, TN, TP	–	1980 to 1989	Daily	0.82	0.72	−3.84%	Impacts of sets of climate and land use change scenarios on water resources
Choi et al. (2017)	2330	Streamflow	–	1986 to 2005	Daily	–	0.70	5%	Impacts of climate change and urban growth on the streamflow
He and Hogue (2012)	1680	Baseflow, peak flow, streamflow	–	1997 to 2006	Daily	0.85	0.69	10.5%	Impact of urbanization on watershed hydrology.
Dudula and Randhir (2016)	401	Streamflow	Bioretention, rain garden	1960 to 2008	Daily	0.73	0.71	–	Modeling the influence of climate change on watershed systems
Fonseca et al. (2014)	176	Temperature, fecal coliforms, TSS, pH	–	2003 to 2006	Daily	0.84	0.84	12.9%	Integrated hydrological and water quality model for river management
Qiu et al. (2018)	3.27	Streamflow, TP, TN, sediment	–	2014 to 2015	Daily	0.90	0.80	–	assessment of watershed-scale NPS pollution during rainfall-runoff events

[a] Low Impact Development.
[b] The coefficient of determination.
[c] Nash-Sutcliffe Efficiency.
[d] Percent bias.
[e] Total Suspended Solids.
[f] Total Nitrogen.
[g] Total Phosphorous.

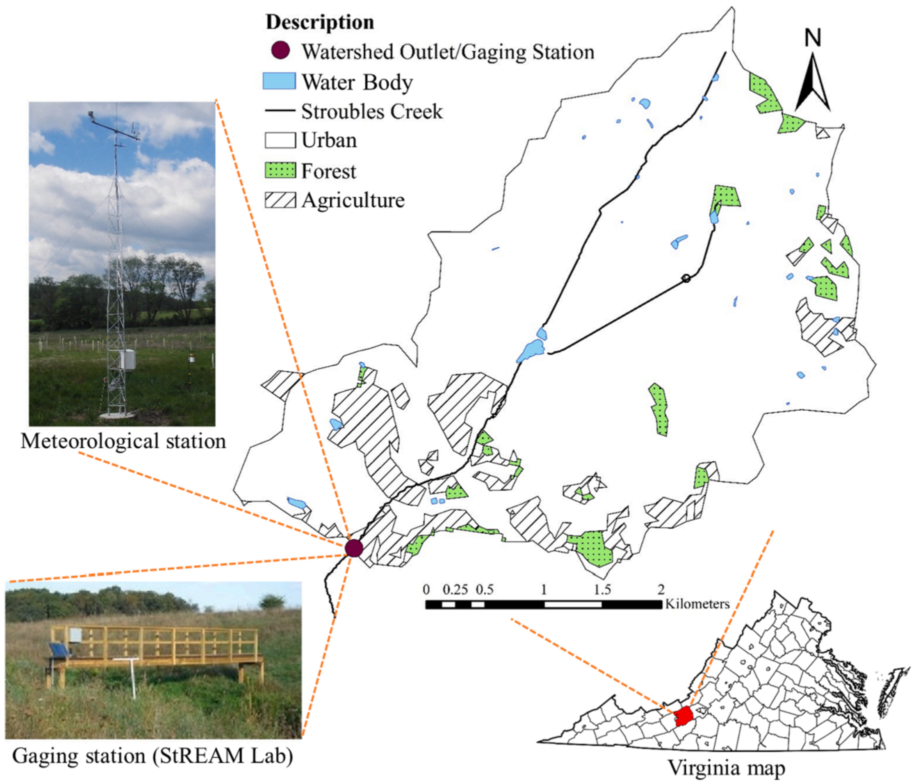

Fig. 1. Land cover types of Stroubles Creek watershed, with gaging and meteorological station locations.

listed in Table 3), depth of unsaturated upper zone and lower saturated zone, aquifer porosity, and saturated hydraulic conductivity (Rossman, 2010). These parameters control flow from the aquifer into the stream (and vice versa) and compute groundwater flow as a function of groundwater and surface water levels. Green-Ampt (GA) infiltration was applied for the infiltration module of SWMM, primarily because the watershed was semi-urbanized and the physical basis of GA parameters such as suction head, hydraulic conductivity, and initial moisture deficit values are available through the Soil Survey Geographic Database (SSURGO). The dynamic wave (DW) algorithm was selected for hydraulic routing within SWMM, because this method can simulate non-uniform and unsteady state flow conditions accurately. The longest flow paths of each subcatchment were used to calculate its hydraulic width (HW), a required SWMM parameter. Excess rainfall that exceeds depression storage is routed from each subcatchment through a nonlinear reservoir algorithm (Macro et al., 2019; Palla and Gnecco, 2015; Xing et al., 2016); each subcatchment is split into pervious and impervious portions, and runoff is directed to a user-defined outlet node or is routed across pervious areas. The Manning's roughness coefficient for pervious and impervious area is used to compute normal flow across a plane (the plane being the subcatchment); these eventually flow into either conveyance piping, ditches, and/or streams, through which flow is calculated by use of the Manning's equation or through culvert formulas which depend upon upstream and downstream conditions.

HSPF includes three principle modules: PERLND (pervious land), IMPLND (impervious land segments), and RCHRES (routing through reaches). Processes in receiving streams can be simulated using the RCHRES (reach and reservoir) module of HSPF. IMPLND module generates surface runoff, whereas the PERLND module analyzes all three major processes including surface runoff, interflow, and groundwater. All processes related to soil infiltration, soil moisture, groundwater, baseflow separation, etc., are analyzed in these modules, enabling HSPF to predict the hydrology and water quality of watersheds (Berndt et al., 2016; Bicknell et al., 2001; Mohamoud and Prieto, 2012; Xu et al., 2007). The PWATER and IWATER sections in HSPF control the water budget allocations between surface flow, interflow, baseflow, storage, interception, detention and evaporation (ET). PWAT-PARM3 is one section of PWATER, which has two parameters of DEEPFR and AGWETP for simulating groundwater recharge. Philips equation (a physically-based method that uses an hourly time step), Chezy-Manning's equation, and kinematic wave (KW) were applied within HSPF for simulating infiltration, streamflow, and hydraulic routing, respectively (Bicknell et al., 2001). Within HSPF, the parameters LZSN and UZSN (Table 3) that control lower and upper zone storage are used to simulate water outflow from streams (Bicknell et al., 2001). The INFLT parameter is an index associated with the Philips infiltration method for quantifying soil infiltration capacity. There are three parameters that control groundwater and baseflow in HSPF; these are KVARY, AGWRC, and DEEPER which are functions of baseflow recession variation and the interactions between groundwater and surface water. BASETP is a parameter that represents the ET of riparian vegetation; when riparian vegetation is present, its value starts with 0.03 (Singh et al., 2005). INTFW and IRC are interflow parameters, which are a function of soil, topography and land use (Bicknell et al., 2001).

The major components of the water balance within the Stroubles Creek watershed include: precipitation, total runoff (sum of overland flow, interflow and baseflow), total actual ET (sum of interception ET, aquifer upper zone ET, aquifer lower zone ET, baseflow ET, and active groundwater ET), and deep groundwater recharge. Each of the aforementioned water balance components have corresponding parameters in SWMM and HSPF (Table 3).

2.4. Baseflow separation

Direct runoff during storm events is the sum of overland flow and interflow, while baseflow consists of groundwater discharge from the saturated zone of an underlying aquifer directly to streams (Lott and Stewart, 2013; Miller et al., 2016; Rumsey et al., 2015). Baseflow affects aquatic habitats during dry periods and low-intensity storm events during periods of high groundwater levels (McCargo and Peterson,

Table 2
Selected attributes of the HSPF and SWMM.

Feature	HSPF (Bicknell et al., 2001)	SWMM (Rossman, 2010)
Weather data	Precipitation, air temperature, solar radiation, cloud cover, wind, dew point, potential evapotranspiration	Precipitation, air temperature, wind speed, evaporation
Flow calibration parameters	20-25 parameters typically use for flow calibration	5-6 parameters typically use for flow calibration
Infiltration	Infiltration is calculated using Philip's equation	SWMM can use Horton or Green-Ampt or Curve number for calculating infiltration,
Water routing	Storage routing or kinematic wave method	Steady flow, Kinematic wave, or dynamic wave
Channel geometry	User-defined	User-defined
Shallow aquifer	Yes	Yes
Deep aquifer	Yes	Yes
LID control	No	Yes
Urban conveyance system	No	Yes

2010). There are several methods to determine and separate baseflow from streamflow, which are grouped into three general categories: graphical, analytical, and mass balance methods (Lott and Stewart, 2016). Baseflow separation partitions a stream hydrograph into baseflow and runoff. The most widely used methods of baseflow separation are analytical (Lott and Stewart, 2016). Eckhardt (2008) developed a two parameters equation through numerical analysis for baseflow separation, which is calculated by Eq. (1).

$$b_k = \frac{(1 - BFI_{\max})ab_{k-1} + (1 - a)BFI \times y_k}{1 - aBFI_{max}} \quad (1)$$

where a is the groundwater recession constant, y is the total streamflow, b is the baseflow, k is the time step, and BFI_{max} is maximum baseflow index. There are three values for maximum baseflow index (BFI_{max}) parameter including 0.80 for perennial streams with porous aquifers, 0.50 for ephemeral streams with porous aquifers, and 0.25 for perennial streams with hard rock aquifers. In this study, a hydrograph analysis tool (Kyoung et al., 2005) was used for baseflow separation, which uses the Eckhardt method (Eckhardt, 2008). The aforementioned method is able to separate baseflow more accurately than other numerical methods, since it utilizes two parameter filters (Eckhardt, 2008; Neff et al., 2005). Since the current stream study is perennial with porous aquifers underneath, a BFI_{max} of 0.80 was used.

2.5. Analysis of storm events

The behavior of each model during storms events with a set return period was assessed. Each calibrated model was used to simulate streamflow for the 1, 2, 5, 10, 25, 50, and 100-year 24-hr precipitation frequency (PF) estimates at the outlet of the Stroubles Creek watershed; the PF estimates were produced by National Oceanic and Atmospheric Administration (NOAA) ATLAS 14 with 90% confidence intervals (NOAA, 2016) using the partial duration time-series type. Natural Resources Conservation Service (NRCS) Type II storm distribution was used to develop time series of 24-hr precipitation events (NRCS, 2015). Groundwater discharge was assumed to be negligible during large storm events. The runoff volume simulated at the outlet of the watershed (by both models) during the 24-hr precipitation was normalized to runoff depth through dividing by the connected impervious area of the watershed. Further, runoff coefficients were calculated as the runoff depth divided by precipitation depth, as, essentially all streamflow was runoff during the event.

2.6. Sensitivity analysis

Sensitivity analysis (SA) is process of the adjusting inputs of a model and calculating the rate of change in model results. SA techniques are grouped into local and global methods (Javaheri et al., 2018). Local SA methods evaluate the sensitivity of parameters around one local point. The value of one particular input parameter was changed while other parameters were held constant during the simulation; hence, the sensitivity of streamflow as the main output of the models to input parameters can be represented by the sensitivity coefficient (Eq. (2)) (James et al., 1982).

Table 3
Selected parameters of HSPF and SWMM based on literature and field review, to assess the sensitivity analysis.

Parameter	Unit	Definition	Function of	Range
HSPF				
LZSN	mm	Lower zone nominal soil moisture storage	Soils, Climate	2.54–381
INFILT	mm/hr.	Index to soil infiltration capacity	Soils, Land use	0.028–25
KVARY	1/mm	Variable groundwater recession flow	Baseflow recession	0–2540
AGWRC	1/day	Groundwater recession rate	Baseflow recession	0.001–0.999
DEEPFR	–	Fraction of inactive groundwater	Geology, Groundwater recharge	0–1
BASETP	–	Baseflow evapotranspiration	Riparian Vegetation	0–1
UZSN	mm	Upper zone Nominal Soil moisture storage	Surface soil conditions, land use	0.254–254
IRC	1/day	Interflow recession parameter	Soils, topography, land use	0.01–0.99
INTFW		Interflow inflow parameter	soils, topography, land use	1–10
SWMM				
HW	m	Hydraulic Width	Longest flow path	± 10% of each subwatershed
IMR	–	Impervious Manning roughness	Soil type, Land use	0.01–0.03
PMR	–	Pervious Manning roughness	Soil type, Land use	0.02–0.45
IDS	mm	Impervious depression storage	Pavement, Land use	0.3–2.3
PDS	mm	Pervious depression storage	Land cover	2.5–5.1
A_1	–	Groundwater flow coefficient	Discharge, Aquifer	0.0001–0.01
B_1	–	Groundwater flow exponent	Discharge, Aquifer	0.0001–1
A_2	–	Surface water flow coefficient	Aquifer	0.0001–0.01
B_2	–	Surface water flow exponent	Aquifer	0.0001–1
CND	mm/day	Conductivity	Soil type	± 20% of initial values

$$S_c = \left(\frac{P}{Y}\right)\left(\frac{Y_1 - Y_2}{P^{max} - P^{min}}\right) \quad (2)$$

where S_c is sensitivity coefficient; P is the input parameter and Y is the predicted output; P^{max} and P^{min} are the maximum and minimum ranges of the initial default value; and Y_1 and Y_2 are the corresponding output values. The most sensitive model parameters in watershed hydrology have higher values of S_c. In addition, Global sensitivity analysis (GSA) techniques evaluate the sensitivity of parameters around the whole parameter space (Dobler and Pappenberger, 2013; Javaheri et al., 2018). The sensitivity analysis identified several key parameters that had a substantial impact on simulation results. The sensitive parameters have the potential to significantly influence SWMM and HSPF simulation results. In applying GSA to the case study, the calibrated value of each model's input parameter was used as the baseline value. Each key model parameter value was varied one at a time, with simulations run for plus and minus 10% of the published range in the parameter value (Table 2). This produced a total spread of 20% in the parameter value, which was assumed to provide a reasonable estimate of inputs. The two simulations produced for the modification of each input parameter provided upper and lower bounds of the simulation results. These limits can be interpreted as error limits of simulation results. This approach is often applied to address the performance evaluation of best management practices (BMPs) and hydrologic models (Janke et al., 2013; Park et al., 2011).

2.7. Calibration and validation

HSPF and SWMM models represent hydrologic and hydraulic features of a watershed using fixed and process-related parameters (Castanedo et al., 2006). Fixed parameters represent the hydraulic features of drainage networks, while physical properties represent drainage basins properties, such as length, slope, width, depth and roughness of a watershed and areas covered by various soil types and land covers. A flow chart describing the process of developing the HSPF and SWMM models in this study is shown in Fig. 2. Process-related parameters cannot normally be measured directly or cannot be calculated through GIS information; these include soil moisture storage, groundwater discharge into stream, ET, etc. (Bicknell et al., 2001; Castanedo et al., 2006). These parameters were adjusted manually during the calibration process between January 1, 2013 and December 30, 2013 for each model using hourly streamflow obtaining from StREAM Lab. There were 22 storm events during calibration period. Validation, which consists of running the models with the calibrated parameters without adjustment, was conducted for the period between January 1, 2009 and December 31, 2012, with 61 storm events. The purpose of model validation is to assess if the calibrated models can simulate streamflow behavior for events outside of the calibration period.

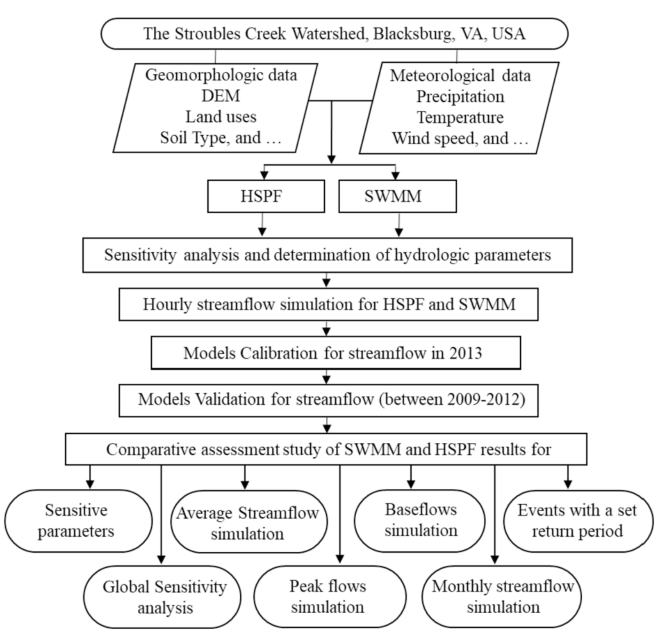

Fig. 2. The flow chart of the application of HSPF-PEST model.

The goodness of fit criteria (for both calibration and validation periods) were investigated using a group of statistical methods including: coefficient of determination (R^2) (Gebremariam et al., 2014; Nasr et al., 2007; Seong et al., 2015), Nash-Sutcliffe Efficiency (NSE) (Nash and Sutcliffe, 1970) and Percent bias (PBIAS) (Gupta et al., 1999). According to Duda et al. (2012) and Moriasi et al. (2015), multiple statistics should be used rather than a single criterion. A model performance rating system, which compared the simulated versus observed datasets qualitatively, was developed to assess model performance (Table 4) (Bennett et al., 2013; Ketabchy et al., 2019; Moriasi et al., 2015; Nayeb Yazdi et al., 2019a). If the statistical parameters showed good or satisfactory agreement (Table 4), the model calibration was considered complete; otherwise, the model calibration parameters were adjusted further. The calibration process stops, when R^2 and NSE are greater than 0.6 and 0.5, respectively, and PBIAS is lower than 0.25% (Fig. 3).

3. Results

3.1. Sensitivity analysis

The results of the local sensitivity analysis for selected input parameters are presented in Table 5. The most sensitive parameters in the HSPF model were groundwater parameters (DEEPFR, AGWRC), followed by INFILT, LZSN parameters, which are functions of soil and land use. The most sensitive parameters of the SWMM model was imperviousness (S_c = 0.38), following by impervious depression storage (S_c = 0.11), and subwatershed hydraulic width (S_c = 0.03). These results are similar to previous studies (Ali and Bruen, 2016; Seong et al., 2015; Tsai et al., 2017; Xing et al., 2016). Compared to HSPF model, the groundwater parameters within SWMM including the groundwater flow coefficient, groundwater flow exponent, surface water flow exponent, and surface water flow coefficient did not substantially affect SWMM results.

3.2. Global sensitivity analysis results

The baseline values of model outputs i.e. average streamflow, average baseflow, and associated variation in modeled outputs are shown in Table 6. GSA was conducted on the most sensitive parameters in HSPF and SWMM, with the upper and lower bounds serving as the extreme endpoints of simulation outputs. During GSA, variability of average streamflow for SWMM was higher than that of HSPF, while variability of average baseflow for HSPF was significantly greater than that of SWMM. The most sensitive parameters of the HSPF model were attributed to groundwater discharge, thus, altering those parameters had direct a significant effect on baseflow. This likely explains why HSPF-simulated baseflow had a larger variability during simulation than similar outputs from the corresponding SWMM model. The sensitive parameters of SWMM were primarily attributed to imperviousness and infiltration, which have a direct effect on runoff and/streamflow (Table 6).

3.3. Comparison of models without calibration

As a baseline for our study, the HSPF and SWMM models were initially run for the entire period of record, without calibration to assess the relative abilities of each model to match the observed data. It

Table 4
Performance assessment of watershed modeling.[a]

Unsatisfactory	Satisfactory	Good	Very good	Statistics
$R^2 \le 0.60$	$0.60 \le R^2 < 0.75$	$0.75 \le R^2 < 0.90$	$0.90 \le R^2 < 1.00$	R^2
NSE ≤ 0.50	0.50 ≤ NSE < 0.65	0.65 ≤ NSE < 0.75	0.75 ≤ NSE < 1.00	NSE
BBIAS ≤ ± 25	± 15 ≤ BBIAS < ± 25	± 10 ≤ BBIAS < ± 15	BBIAS < ± 10	BBIAS

[a] (Duda et al., 2012; Moriasi et al., 2007; Seong et al., 2015; Xu et al., 2007).

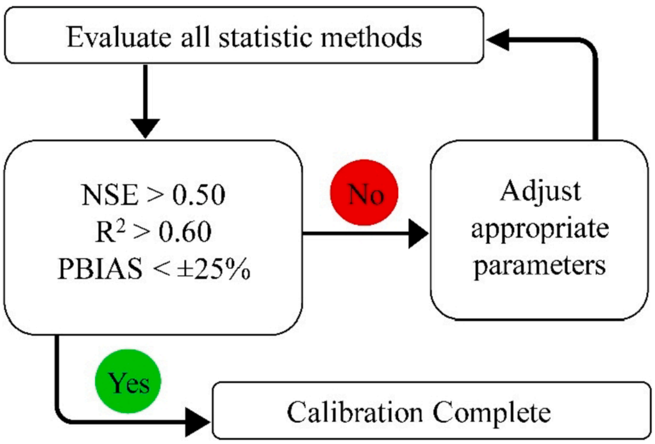

Fig. 3. Diagram of model calibration steps.

Table 5
Ranking of the parameters according to the sensitivities of models output streamflow to them.

Level of sensitivity	Parameter	Sensitivity coefficient (Absolute value)
HSPF		
High	DEEPFR	0.2100
↓	AGWRC	0.0860
Low	INFILT	0.0790
	LZSN	0.0710
	BASETP	0.0250
	UZSN	0.0091
	IRC	0.0028
	INTFW	0.0027
	KVARY	0.0005
SWMM		
High	Imperviousness	0.3800
↓	Impervious depression storage	0.1100
Low		
	Hydraulic width	0.0300
	Pervious Manning's roughness	0.0080
	Conductivity	0.0070

Table 6
Global sensitivity analysis of HSPF and SWMM output simulation results.

Parameter	Average streamflow (m^3/s)	Average baseflow (m^3/s)
HSPF		
Nominal	0.173	0.102
Variation of outputs	0.129 (−25%), 0.181 (+5%)	0.071 (−30%), 0.106 (+4%)
SWMM		
Nominal	0.184	0.088
Variation of outputs	0.129 (−30%), 0.216 (+17)	0.79 (−10%), 0.093 (+5%)

should not be construed that the authors are recommending use of the models without calibration. Our supposition is that SWMM would perform better than HSPF without calibration for the aforementioned reasons. Parameter values for both models were left as estimated from external data sources or model defaults. NSE, R^2, and PBIAS for SWMM was 0.52, 0.58, and −22%, and for HSPF was 0.38, 0.47, and −0.42%, respectively. The results indicated that, without calibration, SWMM simulated streamflow far better than HSPF, earning an "acceptable" vs "poor" according to the metrics by Moriasi et al. (2015). This is due to the finer spatial scale of the inputs to SWMM, which are based more on the externally sourced data such as GIS and the physics of the hydrological processes which control the catchment response, while HSPF is a process-based model that relies on many parameters which can only be determined through calibration. Thus, HSPF is not useful without calibration; whereas SWMM without calibration, while diminished somewhat, may still provide useful information. Thus, HSPF is better for watersheds with monitoring data but only limited physical information, the opposite is the case for SWMM.

3.4. Calibrated input parameters

The calibrated value ranges of input parameters for HSPF and SWMM models are presented in Table 7. The HSPF calibrated input parameters for soil and land use (LZSN, INFILT) were categorized for forest, agricultural, and urban land covers.

Table 7
Selected parameters of HSPF and SWMM for calibration.

Parameter	Unit	Calibrated value/value range
HSPF		
LZSN[a]	mm	381
LZSN[b]	mm	304
LZSN[c]	mm	254
INFILT[a]	mm/hr.	8.350
INFILT[b]	mm/hr.	7.050
INFILT[c]	mm/hr.	5.710
KVARY	1/mm	2.540
AGWRC	1/day	0.990
DEEPFR		0.300
BASETP		0.030
UZSN	mm	50.800
IRC	1/day	0.900
INTFW		5
SWMM		
Hydraulic Width	m	72–1160
Impervious Manning roughness		0.008–0.014
Pervious Manning roughness		0.140–0.218
Imperviousness	%	7.000–68.670
Conductivity	mm/hr.	0.050–34.340

[a] Forest land.
[b] Agricultural land.
[c] Urban land.

Table 8
Goodness-of-fit test results for assessing the reliability of calibration and validation results of HSPF and SWMM model for streamflow.

Parameters	Calibration	Validation	Model Performance Rating[a]
HSPF			
NSE	0.66	0.51	Good/Satisfactory
R^2	0.70	0.64	Satisfactory/Satisfactory
PBIAS	−9.60%	23.40%	Good/Satisfactory
SWMM			
NSE	0.69	0.59	Good/Satisfactory
R^2	0.76	0.74	Satisfactory/Satisfactory
PBIAS	−0.26%	18.20%	Good/Satisfactory

[a] First one represents performance of calibration period and second one indicates that of validation period.

3.5. Comparison of models for average streamflow simulation

Goodness-of-fit results for calibration and validation periods are provided in Table 8. The statistical analysis results showed good agreement between the simulated and observed streamflow. The observed and simulated hydrographs of SWMM and HSPF for calibration and validation periods are shown in Fig. 4. During the calibration and validation periods, SWMM showed slightly better agreement between simulated and observed streamflow than HSPF, based on the statistical values of NSE, R^2, and PBIAS. The positive values of PBIAS for models during validation period indicates the propensity of the models to underestimate streamflow. Since visual comparison of the models results using Fig. 4b was hard to see, two months (i.e. December 2009, and May 2011) were separated for better visualization in a narrower data range (Fig. 4c and d).

Goodness-of-fit was also assessed by plotting the observed vs. simulated values of streamflow in calibration and validation periods as shown in Fig. 5. SWMM calibration replicates many of the storm event peaks reasonably well. The slope of the regression line for the HSPF calibration was less than 1.0 (Fig. 5a), while that of for SWMM calibration period was close to 1.0 (Fig. 5b). Some of the errors are likely due to the inability of the SWMM and HSPF models to capture streamflow peaks for some of the events (Fig. 5a and b). The slope of regression line for validation periods of SWMM and HSPF was approximately 0.7, indicating highly relative magnitude of the residuals to standardized residuals (residuals equal to 0.0). SWMM generally overestimated high magnitude flood events (Fig. 5d), while there was no certain pattern in simulating high magnitude flood events through HSPF (Fig. 5c).

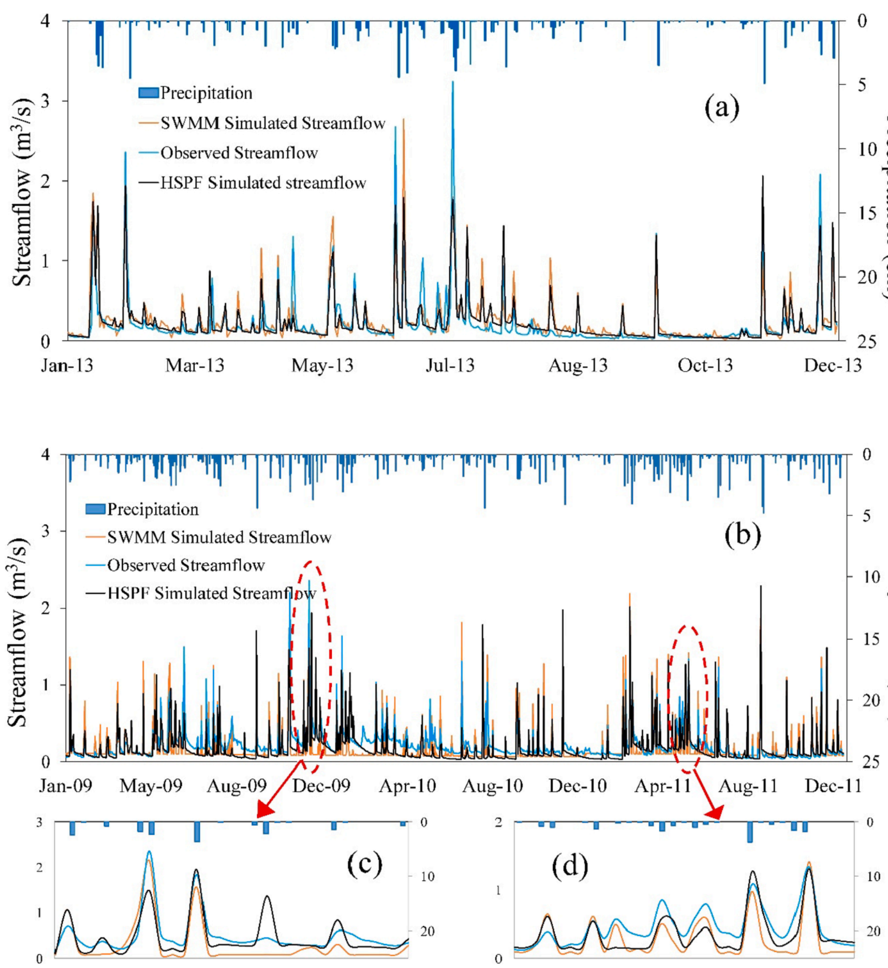

Fig. 4. Comparison of hourly observed and simulated streamflow by HSPF and SWMM for calibration and validation periods (a) Calibration period for 2013 (b) Validation period for 2009–2011 (c) Observed and simulated data for December 2009 (d) Observed and simulated data for May 2011.

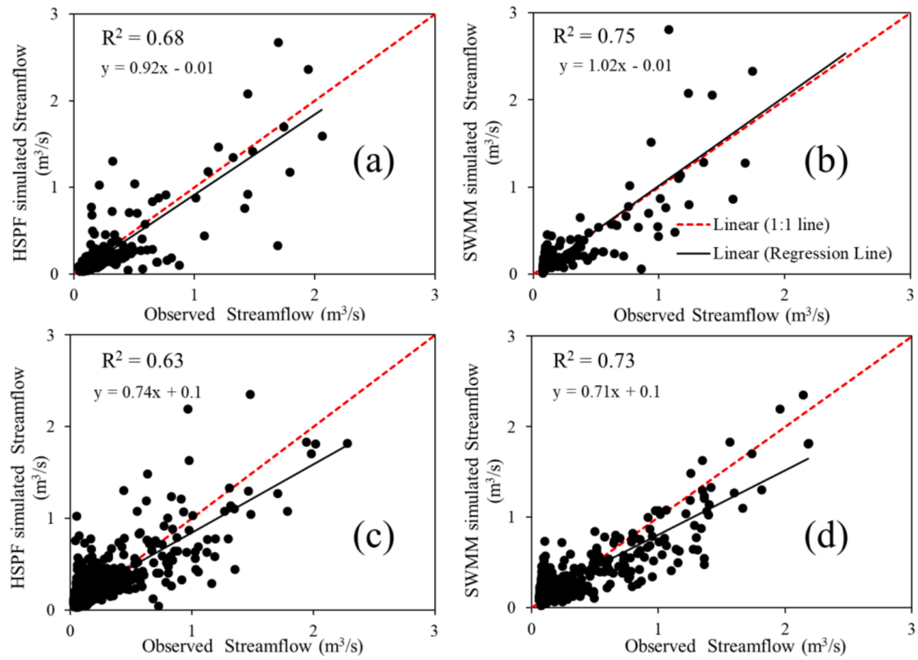

Fig. 5. Scatter plots of observed and simulated streamflow along the 1:1 red line: (a) Calibration for HSPF; (b) Calibration for SWMM; (c) Validation for HSPF; (d) Validation for SWMM.

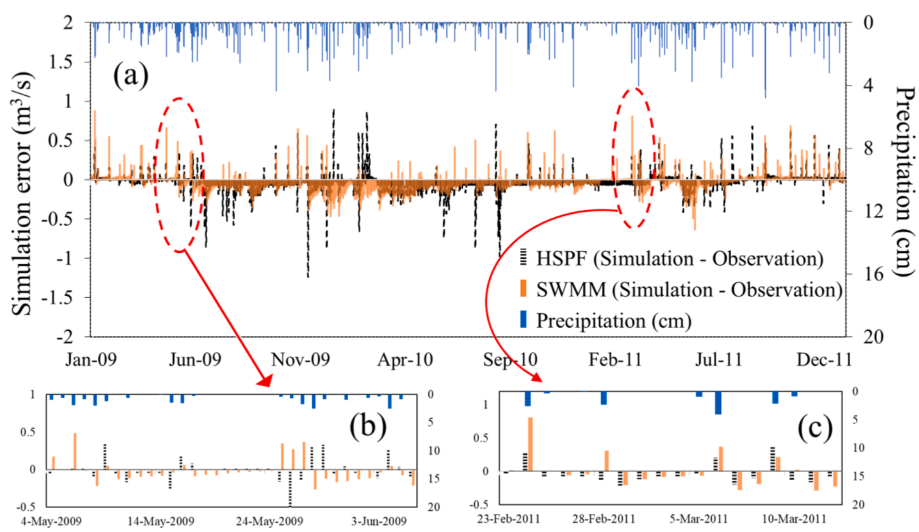

Fig. 6. Comparison of residual error (simulated – observed) for daily streamflow simulation by HSPF and SWMM models (a) Between 2009 and 2012 (b) Between May-2009 to Jun-2009 (c) Between February-2011 to March-2011.

The residual time series of daily streamflow versus time and precipitation is provided in Fig. 6. The HSPF streamflow simulation average error during wet periods (days with at least 0.25 cm precipitation) and dry periods were 0.002 and $-0.067\ m^3/s$, respectively; while those of for SWMM streamflow simulation were 0.067 and $-0.070\ m^3/s$, respectively. The aforementioned analysis indicates relatively better performance of both models in wet period than dry periods (in terms of averaged-error); HSPF appeared to be a better predictor of streamflow in wet periods rather than SWMM. During high magnitude storm events (days with at least 2 cm precipitation), SWMM generally over-estimated the streamflow, while there was no specific pattern for HSPF simulation error.

Flow duration curves of simulated streamflow by HSPF and SWMM and observed streamflow are shown in Fig. 7. Models simulated streamflow close to observed streamflow during high flows (between 0 and 10% flow exceedance Q_{10}). HSPF simulated streamflow between 10% and 90% of flow exceedance were slightly beneath observed streamflow, while SWMM over-predicted streamflow during low flow. Overall, based on a visual look, the HSPF simulation matched better in terms of flow exceedance pattern with observed streamflow compared

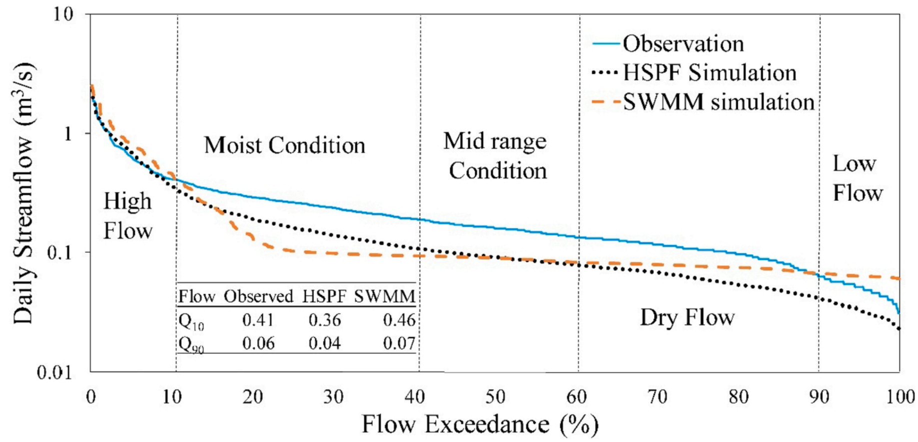

Fig. 7. Comparison of flow duration curves of simulated streamflow by HSPF and SWMM and observed streamflow.

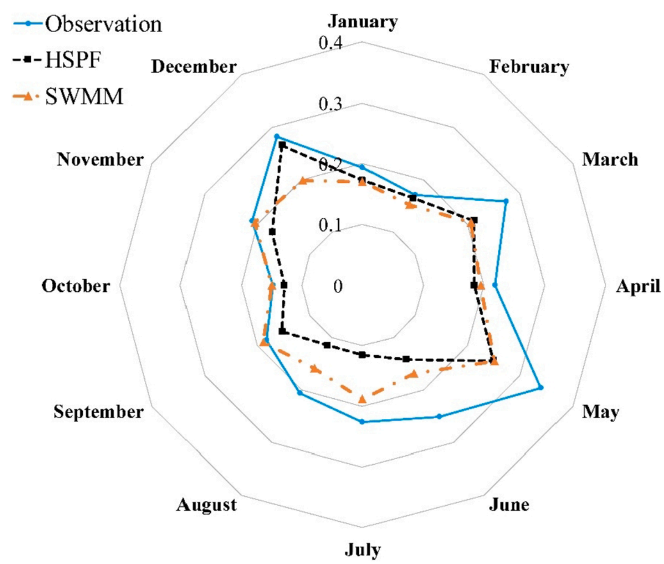

Fig. 8. Radar plot of monthly average of observed and simulated streamflow.

to the SWMM simulation (Fig. 7). The top 10% of streamflow in magnitude (according to Fig. 7) were selected as peak flows to evaluate the capability of HSPF and SWMM in peak flow simulation (there was 81 days of high streamflow for observed dataset). The corresponding PBIAS values of SWMM and HSPF models for peak flow were −0.098 and 0.120, respectively, indicating that SWMM was better at reproducing observed peak flows. The average errors (simulated-observed) of peak flows (7.1% for SWMM and −8.1% for HSPF) confirmed the PBIAS statistical analysis results. The PBIAS values, average percent errors of models, and Fig. 6 represent the overestimation and underestimation of peak flows by SWMM, and HSPF, respectively.

3.6. Comparison of models for monthly streamflow simulation

The average monthly streamflow (representing streamflow seasonally variation) indicated that HSPF and SWMM models achieve better agreement with observed streamflow during winter months (Jan and Feb), rather than summer months (May, Jun, Jul, and Aug) (Fig. 8). The SWMM averaged-percent differences of all months resulted in −15%, while that of for HSPF was −22%, indicating SWMM is a better predictor of seasonally streamflow variation. The percentage difference between the SWMM and HSPF monthly simulated streamflow and the observed monthly streamflow ranged from 6% to 39%, and from 3% to 48%, respectively, which can be classified as not good results for models when PBIAS is higher than 25% (Al-Abed and Al-Sharif, 2008). SWMM performed better than HSPF in summer months, while HSPF simulation matched relatively better with observed averaged-monthly streamflow in winter than SWMM. Generally, both models under-estimated the averaged-monthly streamflow between January 2009 and December 2013 (Fig. 8). The simulation of average monthly streamflow can be beneficial for assessing impact of projected climate and land-use changes.

3.7. Comparison of models for baseflow simulation

The baseflow was plotted as (1) total baseflow and (2) baseflow for dry periods (DPs, or the periods in which precipitation and direct runoff are zero, and groundwater discharge is the only source of streamflow) (Fig. 9). The observed DPs baseflows between 2009 and 2011 was 317 days, while that for SWMM and HSPF simulations were 693, and 199 days, respectively (Fig. 9b); it indicates better performance of HSPF in coverage of the number of dry days period. The PBIAS values of SWMM model for total baseflow and DPs baseflow were 0.4, and 0.61, respectively, while those of for HSPF model were 0.31 and, −0.53, respectively, indicating better performance of HSPF model in capturing observed total baseflow and DPs baseflow. As SWMM and HSPF models were not calibrated through observed baseflow, the aforementioned PBIAS calculations and the respective discussion were only based on baseflow calculation using the Eckhardt (2008) method and the calibrated average streamflow. HSPF captured the observed baseflow pattern better than SWMM model (Fig. 9a and b); in contrast, SWMM followed a relatively constant baseflow pattern throughout the DPs (Fig. 9b). Our results are similar to previous study indicating that SWMM has a limitation concerning baseflow simulation during dry periods, particularly during winter months (Liu et al., 2013).

3.8. Comparison of model response to standard storm events

HSPF and SWMM models were compared during set return period events by running each using standard NRCS 24-h storms. The

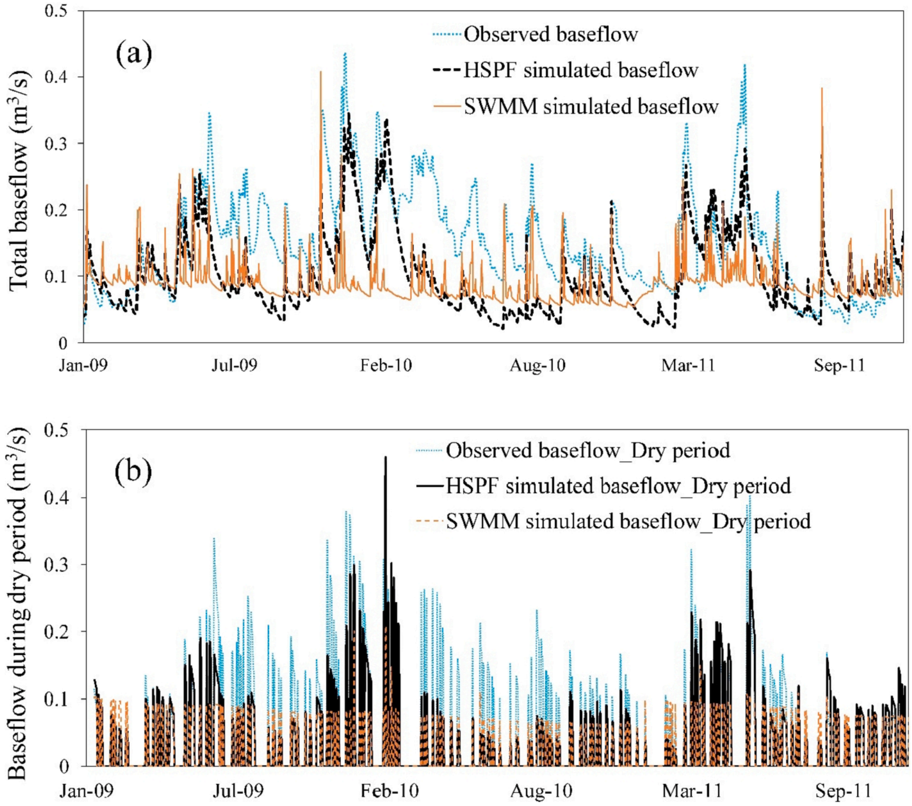

Fig. 9. Comparison of observed, HSPF simulation, and SWMM simulation for total baseflow, and baseflow during dry periods (the periods without precipitation and direct runoff): (a) Total baseflow; (b) baseflow during dry periods.

Blacksburg, Virginia, 1-yr recurrence precipitation is 55 mm (2.2 in) (NOAA, 2016). During the monitoring period, an event (07-July, 2013) was identified and separated and are shown in Fig .10a. During this event, NSE, R^2, and PBIAS between observed and simulated data for SWMM were 0.51, 0.58, and %33, and for HSPF were 0.45, 0.52, and 20%, respectively. Since, the models were calibrated continuously, these results for that event can be can be considered to be acceptable (Moriasi et al., 2015). The simulated hydrograph for 1-yr recurrence interval are presented in Fig. 10b. Results indicated that for extreme storm events SWMM simulated peak flows greater than HSPF, while HSPF simulated higher baseflow than SWMM. SWMM tended to produce more runoff than HSPF for simulated storms with recurrence interval equal or less than 10-yr (Fig. 11). Although the peak flows of SWMM and HSPF 24-hr. storm distribution for the 100-yr. recurrence interval were somewhat similar, a steeper receding limb was evident in the SWMM results compared to HSPF, this accounted for the difference in runoff volume.

4. Discussion

Statistical analysis indicated that both HSPF and SWMM models simulated streamflow adequately. However, the positive values of PBIAS for HSPF and SWMM indicated that both models had a propensity to underestimate streamflow. In addition, the performance of

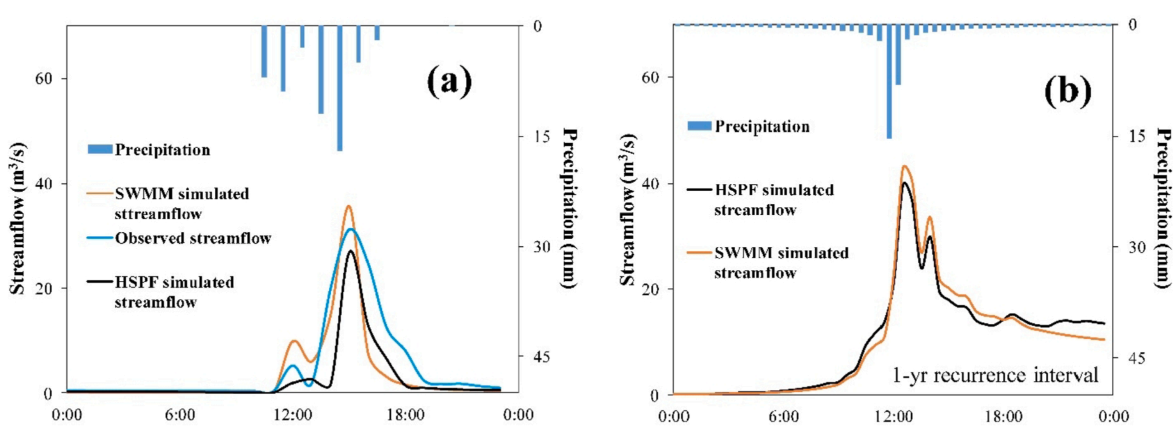

Fig. 10. Comparison of HSPF and SWMM simulation during storm events (a) actual event in 07-July, 2013 (b) artificial 1-yr recurrence interval.

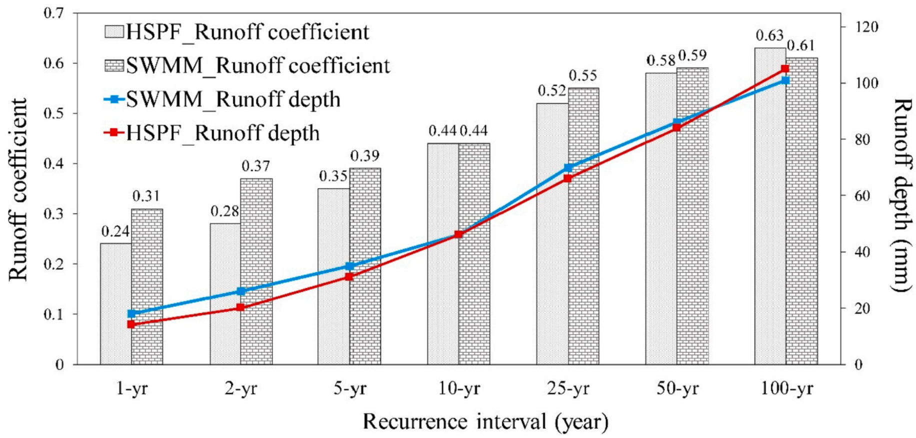

Fig. 11. Predicted runoff depth, and runoff coefficients through SWMM and HSPF modeling tools for the case study watershed.

both models for simulating streamflow during wet periods (days with at least 0.25 cm precipitation) was relatively better than dry periods. It may have been stemmed from the capability of the respective Philips and GA models, which were used for estimating infiltration rate in HSPF and SWMM, respectively. This is because, during storm events, the Philips and GA models estimate infiltration rate relatively better than during dry periods (Chahinian et al., 2005; Wilson, 2017).

During high magnitude storm events (days with at least 2 cm precipitation), SWMM generally over-estimated the streamflow, while there was no specific pattern for HSPF simulation error. HSPF appeared to be a relatively better predictor of streamflow in wet periods rather than SWMM. This may stem from the relative performance of the GA and Philips models, as the Philips infiltration model represented wet periods closer to reality than GA did (Wilson, 2017). In terms of simulating streamflow seasonally, SWMM performed better than HSPF in summer months, while HSPF simulated streamflow better than SWMM in winter.

Generally, the Philip model estimated higher infiltration rates compared to GA (Turner, 2006; Wilson, 2017); this difference could explain the previously mentioned better performance of HSPF in capturing total baseflow and DPs baseflow in comparison to SWMM. Furthermore, HSFP and SWMM use KW and DW methods for runoff/stream routing, respectively. Previous studies indicated that the DW method is more appropriate for obtaining the reference discharge and can capture high flows better than KW (Moramarco et al., 2008; Soentoro, 1991); this may explain why peak flows were better represented by SWMM than HSPF. Overall, the performance difference between HSPF and SWMM in simulating streamflow may be due to the methods were employed for simulating infiltration rate and water routing. These methods resulted in SWMM simulating streamflow better than HSPF within the case study urban watershed. In addition, in the absence of available monitoring data within a watershed, SWMM likely provides better results.

5. Conclusion

Models developed using HSPF and SWMM were used to simulate streamflow for a case study urban watershed, the Stroubles Creek watershed, in Blacksburg, Virginia. Sensitivity analysis was applied only on process-related parameters. Based on sensitivity analysis, the most sensitive hydrologic parameters within HSPF were groundwater parameters i.e. DEEPFR and AGWRC, while for SWMM, it was the percentage of imperviousness. GSA indicated that variation for simulating baseflow-averaged for HSPF was greater than SWMM, while for simulating streamflow, the variability of SWMM outputs was greater than HSPF. SWMM performed better than HSPF sans calibration, due to the inclusion of more detailed watershed topology and SCMs. Analysis of the residual time series of daily streamflow (simulated-observed) indicated that both models performed better during wet rather than dry periods. The comparison results of models for dry periods indicated that HSPF could simulate the total baseflow and DPs baseflow better than SWMM, while the opposite was the case for peak flows. Analysis of extreme storm events was also conducted. The runoff coefficient for SWMM was generally greater than HSPF for recurrence intervals of 1, 2, 5, and 10-yr, and the opposite was true for recurrence intervals greater than 10 years. The results of this study can assist urban watershed planners in translating their results from small scale urban watershed models where SCMs are implemented to larger, regional scale models where compliance is assessed. It can also guide in the selection of the most appropriate model for their urban watershed.

Acknowledgements

Funding for this work was provided in part by the Virginia Agricultural Experiment Station and the Hatch program of the National Institute of Food and Agriculture, U.S. Department of Agriculture, project S1063. The authors appreciate the data provided by Town of Blacksburg, and StREAM Lab with W. Cully Hession and Laura Lehmann, as director and manager, respectively. The authors would like to acknowledge Karen Kline and Adil Godrej (Virginia Tech), and Robert Burgholzer (Virginia Department of Environmental Quality) for their helpful comments.

Appendix A. The geologic map of the Stroubles Creek watershed

The geologic map of the Stroubles Creek Watershed (georeferenced and digitized as a hard copy from the Geology and Mineral Resources Division of Commonwealth of Virginia, 1985) is displayed in Fig. A1. Below are the descriptions concerning characteristics of each geologic type of the watershed.

Td (Talus deposits; the area beneath the ponds of the watershed): Unconsolidated, unsorted boulder fields composed of 0.3–1.8 m thick angular boulders of quartzite, siliceous sandstone and quartzes conglomerate. This detritus has been derived from nearby state of Mississippian, Silurian and Devonian age. Thickness: 0–9.2 m.

Ce (Elbrook Formation): The uppermost part of the formation is characterized by interbedded sandy, commonly crossbed, fine-grain dolomite containing thin (1–10 cm) lenses of fine to medium-grained sandstone and 0.3–1.2 m thick ribbon-banded limestone dolomite.

Cr (Rome Formation; the area mostly at the eastern portion of the watershed): Consists of interbedded mottled, maroon and green phylittic mudstone, fine-grained sandstone and siltstone, and dark-gray, fine-grained dolomite.

Ccr (Copper Ridge Formation; the area upstream of the watershed): inter-bedded medium-gray, fine to medium-grained locally grained, massive dolomite, supper siliceous oolite and quartzose sandstone. Total thickness is about 366 m.

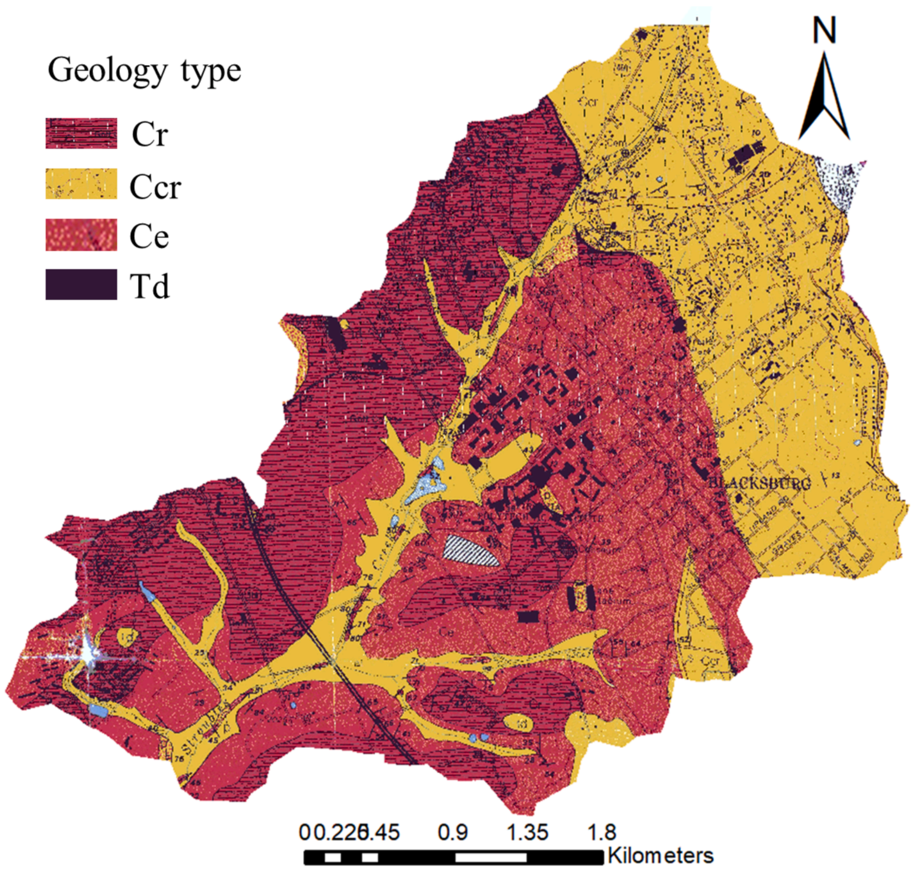

Fig. A.1The geologic map of the Stroubles Creek Watershed.

References

Al-Abed, N., Al-Sharif, M., 2008. Hydrological modeling of Zarqa River Basin - Jordan using the hydrological simulation program - FORTRAN (HSPF) model. Water Resour. Manag. 22, 1203–1220. https://doi.org/10.1007/s11269-007-9221-9.

Alamdari, N., Sample, D., Steinberg, P., Ross, A., Easton, Z., 2017. Assessing the effects of climate change on water quantity and quality in an urban watershed using a calibrated stormwater model. Water 9, 464. https://doi.org/10.3390/w9070464.

Ali, I., Bruen, M., 2016. Methodology and application of the combined SWAT-HSPF model. Environ. Process. 3, 645–661. https://doi.org/10.1007/s40710-016-0167-x.

Bennett, N.D., Croke, B.F.W., Guariso, G., Guillaume, J.H.A., Hamilton, S.H., Jakeman, A.J., Marsili-Libelli, S., Newham, L.T.H., Norton, J.P., Perrin, C., Pierce, S.A., Robson, B., Seppelt, R., Voinov, A.A., Fath, B.D., Andreassian, V., 2013. Characterising performance of environmental models. Environ. Model. Softw 40, 1–20. https://doi.org/10.1016/J.ENVSOFT.2012.09.011.

Berndt, M.E., Rutelonis, W., Regan, C.P., 2016. A comparison of results from a hydrologic transport model (HSPF) with distributions of sulfate and mercury in a mine-impacted watershed in northeastern Minnesota. J. Environ. Manag. 181, 74–79. https://doi.org/10.1016/j.jenvman.2016.05.067.

Bicknell, B.R., Imhoff, J., Kittle Jr., J., Jobes, T., Donigian Jr., A., Johanson, R., 2001. Hydrological Simulation Program–Fortran: HSPF, Version 12 User's Manual. AQUA TERRA Consult. Mt. View, Calif.

Borah, D.K., Ahmadisharaf, E., Padmanabhan, G., Imen, S., Mohamoud, Y.M., 2019. Watershed models for development and implementation of total maximum daily loads. J. Hydrol. Eng. 24https://doi.org/10.1061/(ASCE)HE.1943-5584.0001724. 03118001.

Castanedo, F., Patricio, M. a, Molina, J.M., 2006. Evolutionary computation technique applied to HSPF model calibration of a Spanish watershed BT - 7th international conference on intelligent data engineering and automated learning. IDEAL 216–223 2006, September 20, 2006 - September 23, 2006 4224 LNCS.

Chahinian, N., Moussa, R., Andrieux, P., Voltz, M., 2005. Comparison of infiltration models to simulate flood events at the field scale. J. Hydrol. 306, 191–214. https://doi.org/10.1016/j.jhydrol.2004.09.009.

Chen, J., Theller, L., Gitau, M.W., Engel, B.A., Harbor, J.M., 2017. Urbanization impacts on surface runoff of the contiguous United States. J. Environ. Manag. 187, 470–481. https://doi.org/10.1016/J.JENVMAN.2016.11.017.

Choi, W., Pan, F., Wu, C., 2017. Impacts of climate change and urban growth on the streamflow of the Milwaukee River (Wisconsin, USA). Reg. Environ. Change 17, 889–899. https://doi.org/10.1007/s10113-016-1083-3.

Daghighi, A., 2017. Harmful Algae Bloom Prediction Model for Western Lake Erie Using Stepwise Multiple Regression and Genetic Programming.

Dobler, C., Pappenberger, F., 2013. Global sensitivity analyses for a complex hydrological model applied in an alpine watershed. Hydrol. Process. 27, 3922–3940. https://doi.org/10.1002/hyp.9520.

Duda, P.B., Hummel, P.R., Donigian, A.S.J., Imhoff, J.C., 2012. Basins/HSPF: model use, calibration, and validation. Trans. ASABE (Am. Soc. Agric. Biol. Eng.) 55, 1523–1547. https://doi.org/10.13031/2013.42261.

Dudula, J., Randhir, T.O., 2016. Modeling the influence of climate change on watershed systems: adaptation through targeted practices. J. Hydrol. 541, 703–713. https://doi.org/10.1016/j.jhydrol.2016.07.020.

Eckhardt, K., 2008. A comparison of baseflow indices, which were calculated with seven different baseflow separation methods. J. Hydrol. 352, 168–173. https://doi.org/10.1016/j.jhydrol.2008.01.005.

Fonseca, A., Botelho, C., Boaventura, R.A.R., Vilar, V.J.P., 2014. Integrated hydrological and water quality model for river management: a case study on Lena River. Sci. Total Environ. 485–486, 474–489. https://doi.org/10.1016/j.scitotenv.2014.03.111.

Gebremariam, S.Y., Martin, J.F., DeMarchi, C., Bosch, N.S., Confesor, R., Ludsin, S.A., 2014. A comprehensive approach to evaluating watershed models for predicting river flow regimes critical to downstream ecosystem services. Environ. Model. Softw 61, 121–134. https://doi.org/10.1016/j.envsoft.2014.07.004.

Golden, H.E., Hoghooghi, N., 2017. Green infrastructure and its catchment-scale effects: an emerging science. Wiley Interdiscip. Rev. Water 5https://doi.org/10.1002/wat2.1254. e1254.

Guan, M., Sillanpää, N., Koivusalo, H., 2015. Modelling and assessment of hydrological changes in a developing urban catchment. Hydrol. Process. 29, 2880–2894. https://doi.org/10.1002/hyp.10410.

Gupta, H.V., Sorooshian, S., Yapo, P.O., 1999. Status of automatic calibration for hydrologic models: comparison with multilevel expert calibration. J. Hydrol. Eng. 4, 135–143. https://doi.org/10.1061/(ASCE)1084-0699(1999)4:2(135).

He, M., Hogue, T.S., 2012. Integrating hydrologic modeling and land use projections for evaluation of hydrologic response and regional water supply impacts in semi-arid environments. Environ. Earth Sci. 65, 1671–1685. https://doi.org/10.1007/s12665-011-1144-3.

Hester, E.T., Bauman, K.S., 2013. Stream and retention pond thermal response to heated summer runoff from urban impervious surfaces. J. Am. Water Resour. Assoc. 49, 328–342. https://doi.org/10.1111/jawr.12019.

Hofmeister, K.L., Cianfrani, C.M., Hession, W.C., 2015. Complexities in the stream temperature regime of a small mixed-use watershed, Blacksburg, VA. Ecol. Eng. 78, 101–111. https://doi.org/10.1016/J.ECOLENG.2014.05.019.

Huber, W.C., Dickinson, R.E., 1988. Storm Water Management Model , Version 4 : User's Manual 720. EPA/600/3-88/001a.

Huiliang, W., Zening, W., Caihong, H., Xinzhong, D., 2015. Water and nonpoint source pollution estimation in the watershed with limited data availability based on hydrological simulation and regression model. Environ. Sci. Pollut. Res. 22, 14095–14103. https://doi.org/10.1007/s11356-015-4450-6.

James, L., Burges, S., Johnson, H.P., Brakensiek, D.L., 1982. Selection, Calibration, and Testing of Hydrologic Models, Hydrologic Modeling of Small Watersheds CT Haan. Mich, Joseph, pp. 437–472.

James, W., Rossman, L.A., James, W.R., 2010. User's Guide to SWMM5.

Janke, B.D., Herb, W.R., Mohseni, O., Stefan, H.G., 2013. Case study of simulation of heat export by rainfall runoff from a small urban watershed using MINUHET. J. Hydrol. Eng. 18, 995–1006.

Javaheri, A., Babbar-Sebens, M., Alexander, J., Bartholomew, J., Hallett, S., 2018. Global sensitivity analysis of water age and temperature for informing salmonid disease management. J. Hydrol. 561, 89–97. https://doi.org/10.1016/J.JHYDROL.2018.02.053.

Ketabchy, M., 2018. Thermal Evaluation of an Urbanized Watershed Using SWMM and MINUHET : a Case Study of the Stroubles Creek Watershed. pp. 1–117. Blacksburg , VA (in na). https://doi.org/10.13140/RG.2.2.26726.47688.

Ketabchy, M., Sample, D.J., Wynn-Thompson, T., Nayeb Yazdi, M., 2018. Thermal evaluation of urbanization using a hybrid approach. J. Environ. Manag. 226, 457–475. https://doi.org/10.1016/J.JENVMAN.2018.08.016.

Ketabchy, M., Sample, D.J., Wynn-Thompson, T., Yazdi, M.N., 2019. Simulation of watershed-scale practices for mitigating stream thermal pollution due to urbanization. Sci. Total Environ. 671, 215–231. https://doi.org/10.1016/J.SCITOTENV.2019.03.248.

Kyoung, J.L., Engel, B.A., Tang, Z., Choi, J., Kim, K.S., Muthukrishnan, S., Tripathy, D., 2005. Automated Web GIS based hydrograph analysis tool, WHAT. J. Am. Water Resour. Assoc. 41, 1407–1416. https://doi.org/10.1111/j.1752-1688.2005.tb03808.x.

Lacher, I.L., Ahmadisharaf, E., Fergus, C., Akre, T., Mcshea, W.J., Benham, B.L., Kline, K.S., 2019. Scale-dependent impacts of urban and agricultural land use on nutrients, sediment, and runoff. Sci. Total Environ. 652, 611–622. https://doi.org/10.1016/J.SCITOTENV.2018.09.370.

Lee, S.-B., Yoon, C.-G., Jung, K.W., Hwang, H.S., 2010. Comparative evaluation of runoff and water quality using HSPF and SWMM. Water Sci. Technol. 62, 1401. https://doi.org/10.2166/wst.2010.302.

Li, H., Harvey, J.T., Holland, T.J., Kayhanian, M., 2013. Corrigendum: the use of reflective and permeable pavements as a potential practice for heat island mitigation and stormwater management. Environ. Res. Lett. 8https://doi.org/10.1088/1748-9326/8/4/049501. 049501.

Liao, H., Krometis, L.-A., Kline, K., Hession, W., 2015. Long-Term impacts of bacteria–sediment interactions in watershed-scale microbial fate and transport modeling. J. Environ. Qual. 44, 1483–1490. https://doi.org/10.2134/jeq2015.03.0169.

Linsley, R.K., Kohler, M.A., Paulhus, J., 1975. Hydrology For Engineers, second ed. McGraw-Hill, New York.

Liu, A., Goonetilleke, A., Egodawatta, P., 2015. Role of Rainfall and Catchment Characteristicson Urban Stormwater Quality.

Liu, G., Schwartz, F.W., Kim, Y., 2013. Complex baseflow in urban streams: an example from central Ohio, USA. Environ. Earth Sci. 70, 3005–3014. https://doi.org/10.1007/s12665-013-2358-3.

Liu, J., Shen, Z., Chen, L., 2018. Assessing how spatial variations of land use pattern affect water quality across a typical urbanized watershed in Beijing, China. Landsc. Urban Plan. 176, 51–63. https://doi.org/10.1016/j.landurbplan.2018.04.006.

Locatelli, L., Mark, O., Mikkelsen, P.S., Arnbjerg-Nielsen, K., Deletic, A., Roldin, M., Binning, P.J., 2017. Hydrologic impact of urbanization with extensive stormwater infiltration. J. Hydrol. 544, 524–537. https://doi.org/10.1016/J.JHYDROL.2016.11.030.

Lott, D.A., Stewart, M.T., 2016. Base flow separation: a comparison of analytical and mass balance methods. J. Hydrol. 535, 525–533. https://doi.org/10.1016/j.jhydrol.2016.01.063.

Lott, D.A., Stewart, M.T., 2013. A power function method for estimating base flow. Gr. Water 51, 442–451. https://doi.org/10.1111/j.1745-6584.2012.00980.x.

Lucas, W.C., Sample, D.J., 2015. Reducing combined sewer overflows by using outlet controls for Green Stormwater Infrastructure: case study in Richmond, Virginia. J. Hydrol. 520, 473–488. https://doi.org/10.1016/j.jhydrol.2014.10.029.

Luo, K., Hu, X., He, Q., Wu, Z., Cheng, H., Hu, Z., Mazumder, A., 2018. Impacts of rapid urbanization on the water quality and macroinvertebrate communities of streams: a case study in Liangjiang New Area, China. Sci. Total Environ. 621, 1601–1614. https://doi.org/10.1016/J.SCITOTENV.2017.10.068.

Macro, K., Matott, L.S., Rabideau, A., Ghodsi, S.H., Zhu, Z., 2019. OSTRICH-SWMM: a new multi-objective optimization tool for green infrastructure planning with SWMM. Environ. Model. Softw 113, 42–47. https://doi.org/10.1016/J.ENVSOFT.2018.12.004.

McCargo, J.W., Peterson, J.T., 2010. An evaluation of the influence of seasonal base flow and geomorphic stream characteristics on coastal plain stream fish assemblages. Trans. Am. Fish. Soc. 139, 29–48. https://doi.org/10.1577/T09-036.1.

Miller, M.P., Buto, S.G., Susong, D.D., Rumsey, C.A., 2016. The importance of base flow in sustaining surface water flow in the Upper Colorado River Basin. Water Resour. Res. 52, 3547–3562. https://doi.org/10.1002/2015WR017963.

Mohamoud, Y.M., Parmar, R., Wolfe, K., 2010. Modeling best management practices (BMPs) with HSPF. In: Watershed Management 2010. American Society of Civil Engineers, Reston, VA, pp. 892–898. https://doi.org/10.1061/41143(394)81.

Mohamoud, Y.M., Prieto, L.M., 2012. Effect of temporal and spatial rainfall resolution on hspf predictive performance and parameter estimation. J. Hydrol. Eng. 17, 377–388. https://doi.org/10.1061/(ASCE)HE.1943-5584.0000457.

Moore, M.F., Vasconcelos, J.G., Zech, W.C., 2017. Modeling highway stormwater runoff and groundwater table variations with SWMM and GSSHA. J. Hydrol. Eng. 22https://doi.org/10.1061/(ASCE)HE.1943-5584.0001537. 04017025.

Moramarco, T., Pandolfo, C., Singh, V.P., 2008. Accuracy of kinematic wave approximation for flood routing. II. Unsteady analysis. J. Hydrol. Eng. 13, 1089–1096. https://doi.org/10.1061/(ASCE)1084-0699(2008)13:11(1089).

Moriasi, D.N., Arnold, J.G., Van Liew, M.W., Binger, R.L., Harmel, R.D., Veith, T.L., 2007. Model evaluation guidelines for systematic quantification of accuracy in watershed simulations. Trans. ASABE (Am. Soc. Agric. Biol. Eng.) 50, 885–900. https://doi.org/10.13031/2013.23153.

Moriasi, D.N., Gitau, M.W., Pai, N., Daggupati, P., 2015. Hydrologic and water quality models: performance measures and evaluation criteria. Trans. ASABE (Am. Soc. Agric. Biol. Eng.) 58, 1763–1785. https://doi.org/10.13031/trans.58.10715.

Mostaghimi, S., Benham, B., Brannan, K., Dillaha, T.A., Wagner, R., Wynn, J., G, Y, Zeckoski, R., 2003. Benthic TMDL for Stroubles Creek in Montgomery County. (Virginia).

Multi-Resolution Land Use Consortium, 2011. Multi-resolution land use Consortium national land cover Database (NLCD). https://doi.org/http://www.mrlc.gov/nlcd11_data.php.

Nash, J.E., Sutcliffe, J.V., 1970. River flow forecasting through conceptual models part I — a discussion of principles. J. Hydrol. 10, 282–290. https://doi.org/10.1016/0022-1694(70)90255-6.

Nasr, A., Bruen, M., Jordan, P., Moles, R., Kiely, G., Byrne, P., 2007. A comparison of SWAT, HSPF and SHETRAN/GOPC for modelling phosphorus export from three catchments in Ireland. Water Res. 41, 1065–1073. https://doi.org/10.1016/j.watres.2006.11.026.

Nayeb Yazdi, M., Arhami, M., Delavarrafiee, M., Ketabchy, M., 2019a. Developing air exchange rate models by evaluating vehicle in-cabin air pollutant exposures in a highway and tunnel setting: case study of Tehran, Iran. Environ. Sci. Pollut. Res. 1, 501–513. https://doi.org/10.1007/s11356-018-3611-9.

Nayeb Yazdi, M., Sample, D.J., Scott, D., Owen, J.S., Ketabchy, M., Alamdari, N., 2019b. Water quality characterization of storm and irrigation runoff from a container nursery. Sci. Total Environ. 667, 166–178. https://doi.org/10.1016/j.scitotenv.2019.02.326.

Neff, B.P., Day, S.M., Piggott, A.R., Fuller, L.M., 2005. Base flow in the great lakes basin. U.S. Geol. Surv. Sci. Investig. Rep. 32.

Niazi, M., Nietch, C., Maghrebi, M., 2017. Stormwater management model: performance review and gap analysis. J. Sustain. Water Built Environ. https://doi.org/10.1061/JSWBAY.0000817.

NOAA, 2016. Precipitation Frequency. Data Server [WWW Document]. Natl. Ocean. Atmos. Adm. URL https://hdsc.nws.noaa.gov/hdsc/pfds.

NRCS, 2015. Storm Rainfall Depthand Distribution. Natural Resources Conservation Service.

NRCS, 2007. National Engineering Handbook Chapter 7 Hydrologic Soil Groups. United States Department of Agriculture. https://directives.sc.egov.usda.gov/OpenNonWebContent.aspx?content=17757.wba.

NRCS, 1999. SSURGO. https://websoilsurvey.sc.egov.usda.gov/App/HomePage.htm.

NRCS, 1999. Natural Resources Conservation Service. [WWW Document]. United States Dep. Agric. URL https://websoilsurvey.sc.egov.usda.gov/App/HomePage.htm.

Palla, A., Gnecco, I., 2015. Hydrologic Modeling of Low Impact Development Systems at the Urban Catchment Scale. https://doi.org/10.1016/j.jhydrol.2015.06.050.

Park, D., Loftis, J.C., Roesner, L.A., 2011. Performance modeling of storm water best management practices with uncertainty analysis. J. Hydrol. Eng. 16, 332–344. https://doi.org/10.1061/(ASCE)HE.1943-5584.0000323.

Qiu, J., Shen, Z., Wei, G., Wang, G., Xie, H., Lv, G., 2018. A systematic assessment of watershed-scale nonpoint source pollution during rainfall-runoff events in the Miyun Reservoir watershed. Environ. Sci. Pollut. Res. 25, 6514–6531. https://doi.org/10.1007/s11356-017-0946-6.

Rai, P.K., Chahar, B.R., Dhanya, C.T., 2017. GIS-based SWMM model for simulating the catchment response to flood events. Nord. Hydrol 48, 384–394. https://doi.org/10.2166/nh.2016.260.

Roodsari, B.K., Chandler, D.G., 2017. Distribution of surface imperviousness in small urban catchments predicts runoff peak flows and stream flashiness. Hydrol. Process. 31, 2990–3002. https://doi.org/10.1002/hyp.11230.

Rosa, D.J., Clausen, J.C., Dietz, M.E., 2015. Calibration and verification of SWMM for low impact development. JAWRA J. Am. Water Resour. Assoc. 51, 746–757. https://doi.org/10.1111/jawr.12272.

Rosburg, T.T., Nelson, P.A., Bledsoe, B.P., 2017. Effects of urbanization on flow duration and stream flashiness: a case study of puget sound streams, western Washington,

USA. JAWRA J. Am. Water Resour. Assoc. 53, 493–507. https://doi.org/10.1111/1752-1688.12511.
Rossman, L.A., 2010. Storm Water Management Model User's Manual, Version 5.0. National Risk Management Research Laboratory, Office of Research and Development, US Environmental Protection Agency, Cincinnati.
Rumsey, C.A., Miller, M.P., Susong, D.D., Tillman, F.D., Anning, D.W., 2015. Regional scale estimates of baseflow and factors influencing baseflow in the Upper Colorado River Basin. J. Hydrol. Reg. Stud. 4, 91–107. https://doi.org/10.1016/J.EJRH.2015.04.008.
Seong, C., Herand, Y., Benham, B.L., 2015. Automatic calibration tool for hydrologic simulation program-FORTRAN using a shuffled complex evolution algorithm. Water (Switzerland) 7, 503–527. https://doi.org/10.3390/w7020503.
Shenk, G.W., Wu, J., Linker, L.C., 2012. Enhanced HSPF model structure for Chesapeake Bay watershed simulation. J. Environ. Eng. 138, 949–957. https://doi.org/10.1061/(ASCE)EE.1943-7870.0000555.
Singh, J., Knapp, H.V., Arnold, J.G., Demissie, M., 2005. Hydrological modeling of the iroquois river watershed using HSPF and SWAT. J. Am. Water Resour. Assoc. 41, 343–360. https://doi.org/10.1111/j.1752-1688.2005.tb03740.x.
Soentoro, E., 1991. Comparison of Flood Routing Methods. Doctoral dissertation, University of British Columbia. http://resolver.ebscohost.com/openurl?url_ver=Z39.88-2004&rft_val_fmt=info:ofi/fmt:kev:mtx:journal&_char_set=utf8&rft_id=info:doi/10.14288/1.0050451&rfr_id=info:sid/libx%3Avirginiatech&rft.genre=article.
Stern, M., Flint, L., Minear, J., Flint, A., Wright, S., 2016. Characterizing changes in streamflow and sediment supply in the sacramento River Basin, California, using Hydrological Simulation Program-FORTRAN (HSPF). Water (Switzerland) 8. https://doi.org/10.3390/w8100432.
Stoner, E.W., Arrington, D.A., 2017. Nutrient inputs from an urbanized landscape may drive water quality degradation. Sustain. Water Qual. Ecol. 9 (10), 136–150. https://doi.org/10.1016/J.SWAQE.2017.11.001.
StREAM Lab, 2009. Stream research, education, and management Lab (StREAM Lab), Virginia Tech. https://www.bse.vt.edu/research/facilities/StREAM_Lab.html.
Tong, S.T.Y., Sun, Y., Ranatunga, T., He, J., Yang, Y.J., 2012. Predicting plausible impacts of sets of climate and land use change scenarios on water resources. Appl. Geogr. 32, 477–489. https://doi.org/10.1016/J.APGEOG.2011.06.014.
Town of Blacksburg, 2015. Blacksburg GIS Database. http://www.gis.lib.vt.edu/gis_data/Blacksburg/GISPage.html.
Tsai, L.-Y., Chen, C.-F., Fan, C.-H., Lin, J.-Y., 2017. Using the HSPF and SWMM models in a high pervious watershed and estimating their parameter sensitivity. Water 9, 780. https://doi.org/10.3390/w9100780.
Turner, E.R., 2006. Comparison of Infiltration Equations and T Heir Field Validation with Rainfall Simulation 202.
U.S.EPA, 2014. HSPF BMP Web Toolkit: Ecosystems Research Division. http://www.epa.gov/athens/research/modeling/HSPFWebTools/ [WWW Document]. Environ. Prot. Agency. URL.
USEPA, 2018. Storm Water Management Model (SWMM). [WWW Document]. URL. https://www.epa.gov/water-research/storm-water-management-model-swmm 1.11.19.
USEPA, 2014. Hydrological Simulation Program - FORTRAN (HSPF).
USEPA, 2010. Chesapeake Bay Phase 5 Community Watershed Model. U.S Environ. Prot. Agency [WWW Document].
Whitney, J.W., Glancy, P.A., Buckingham, S.E., Ehrenberg, A.C., 2015. Effects of rapid urbanization on streamflow, erosion, and sedimentation in a desert stream in the American Southwest. Anthropocene 10, 29–42. https://doi.org/10.1016/J.ANCENE.2015.09.002.
Wilson, R.L., 2017. Comparing Infiltration Models to Estimate Infiltration Potential at Henry V Events. Portland State University. http://pdxscholar.library.pdx.edu/cgi/viewcontent.cgi?article=1514&context=honorstheses.
Xing, W., Li, P., Cao, S., Gan, L., Liu, F., Zuo, J., 2016. Layout effects and optimization of runoff storage and filtration facilities based on SWMM simulation in a demonstration area. Water Sci. Eng. 9, 115–124. https://doi.org/10.1016/j.wse.2016.06.007.
Xu, Z., Godrej, A.N., Grizzard, T.J., 2007. The hydrological calibration and validation of a complexly-linked watershed-reservoir model for the Occoquan watershed, Virginia. J. Hydrol. 345, 167–183. https://doi.org/10.1016/j.jhydrol.2007.07.015.
Yousefi, S., Moradi, H.R., Keesstra, S., Pourghasemi, H.R., Navratil, O., Hooke, J., 2017. Effects of urbanization on river morphology of the Talar river, mazandarn province, Iran. Geocarto Int. 1–17. https://doi.org/10.1080/10106049.2017.1386722.
Zope, P.E., Eldho, T.I., Jothiprakash, V., 2016. Impacts of land use–land cover change and urbanization on flooding: a case study of Oshiwara River Basin in Mumbai, India. Catena 145, 142–154. https://doi.org/10.1016/J.CATENA.2016.06.009.